Insect Systematics and Diversity, (2021) 5(5): 3; 1–15
doi: 10.1093/isd/ixab012
Research

Evolution

Divergence in Body Mass, Wing Loading, and Population Structure Reveals Species-Specific and Potentially Adaptive Trait Variation Across Elevations in Montane Bumble Bees

Jeffrey D. Lozier,[1,5] Zachary M. Parsons,[2] Lois Rachoki,[2] Jason M. Jackson,[1] Meaghan L. Pimsler,[1] Kennan J. Oyen,[2,3] James Strange,[4] and Michael E. Dillon[2]

[1]Department of Biological Sciences, The University of Alabama, Box 870344 Tuscaloosa, AL 35487, USA, [2]Department of Zoology & Physiology and Program in Ecology, University of Wyoming, Laramie, WY 82072, USA, [3]Department of Biological Sciences, University of Cincinnati, 318 College Drive, Cincinnati, OH 45221, USA, [4]Department of Entomology, The Ohio State University, 216 Kottman Hall, 2021 Coffey Road, Columbus, OH 43210-1132, USA, and [5]Corresponding author, tel: +1 205-348-2754, e-mail: jlozier@ua.edu

Subject Editor: Heather Hines

Received 21 January 2021; Editorial decision 8 April 2021

Abstract

Biogeographic clines in morphology along environmental gradients can illuminate forces influencing trait evolution within and between species. Latitude has long been studied as a driver of morphological clines, with a focus on body size and temperature. However, counteracting environmental pressures may impose constraints on body size. In montane landscapes, declines in air density with elevation can negatively impact flight performance in volant species, which may contribute to selection for reduced body mass despite declining temperatures. We examine morphology in two bumble bee (Hymenoptera: Apidae: *Bombus* Latreille) species, *Bombus vancouverensis* Cresson and *Bombus vosnesenskii* Radoszkowski, across mountainous regions of California, Oregon, and Washington, United States. We incorporate population genomic data to investigate the relationship between genomic ancestry and morphological divergence. We find that *B. vancouverensis*, which tends to be more specialized for high elevations, exhibits stronger spatial-environmental variation, being smaller in the southern and higher elevation parts of its range and having reduced wing loading (mass relative to wing area) at high elevations. *Bombus vosnesenskii*, which is more of an elevational generalist, has substantial trait variation, but spatial-environmental correlations are weak. Population structure is stronger in the smaller *B. vancouverensis*, and we find a significant association between elevation and wing loading after accounting for genetic structure, suggesting the possibility of local adaptation for this flight performance trait. Our findings suggest that some conflicting results for body size trends may stem from distinct environmental pressures that impact different aspects of bumble bee ecology, and that different species show different morphological clines in the same region.

Key words: wing loading, Bergmann's rule, elevation, thermoregulation

Body size is a fundamental trait that drives multiple aspects of organismal physiology, ecology, and evolution, and there has long been interest in the spatial and environmental factors that drive size variation within and between species (Bergmann 1847, Mayr 1956, Chown and Gaston 2010). Gradients in temperature have been implicated most often in body size variation owing to heat conservation benefits, producing the hallmark trend of increasing body size with latitude (i.e., Bergmann's rule) (Ashton 2002). Originally intended to describe body size patterns among species of endothermic animals (Ashton 2002), Bergmann's rule has been expanded to studies of adaptation within species (Mayr 1956, James 1970, Ashton et al. 2000, Ashton 2002) and to organisms like insects and other ectotherms (Ashton and Feldman 2003). The generality of these trends and their sensitivity to confounding environmental factors remains debated, however (Ashton 2001, Dillon et al. 2006, Chown and Gaston 2010, Shelomi 2012). Taxonomic group and life history strategy (e.g., endothermy vs ectothermy) can influence responses to temperature gradients, and for some groups, especially insects, inverse or absent Bergmann clines are typical (Blanckenhorn and Demont 2004, Shelomi 2012, Gérard et al. 2018). Even when Bergmann clines are identified, thermoregulation and heat conservation are not always the best explanations (Ashton et al. 2000, Angilletta et al. 2004, Blanckenhorn and Demont 2004), and spurious Bergmann's clines produced by alternative abiotic factors are possible.

One possible explanation for conflicting data on Bergmann's rule is that morphological clines might be obfuscated when species inhabit environmentally and spatially heterogeneous landscapes. For example, organisms that occur across montane habitats may face competing selective pressures that have shaped morphological variation (Dillon et al. 2006). Declines in temperature with elevation (~6°/km) may parallel temperature declines with latitude and could conceivably produce parallel body size clines (Horne et al. 2018). However, other abiotic factors like air density and oxygen decrease with elevation and may impose unique trade-offs for thermoregulation and locomotion in flying species that range across both latitude and altitude (Altshuler et al. 2004, Dillon and Frazier 2006, Dillon et al. 2006). Whereas cold temperatures at high elevations might select for larger body sizes due to heat conservation, reduced air density at high elevations challenges flight, potentially selecting for reduced body size and, in particular, reduced wing loading (the ratio of body mass to wing area). By having larger wings relative to body size (i.e., reduced wing loading), flying animals decrease induced power requirements, thereby minimizing the energetic costs of flight (Dudley 2000), particularly when challenged by reduced air density (Altshuler et al. 2004). Smaller insects tend to have lower wing loading, driven by hypometric scaling of wing area with body mass, and might thus have an advantage at high elevations (Dillon and Dudley 2004; Dillon et al. 2006, Dillon and Frazier 2006). Reduced oxygen availability at high altitudes could also contribute to selection for smaller size. The gradient between atmospheric and internal oxygen partial pressure (PO_2) is the driving force for oxygen delivery; reduced atmospheric PO_2, therefore, challenges oxygen delivery, particularly in larger insects (Harrison et al. 2010, 2018b; Vogt and Dillon 2013; Nijhout and Callier 2015). Thin air at altitude may, therefore, select for smaller size or for disproportionate increases in wing size for heavier organisms. Comparison of multiple traits that relate to both thermoregulation (e.g., body mass) and flight (e.g., wing loading and oxygen delivery) across multiple spatial dimensions may thus be needed to reveal how body size evolves across complex landscapes for volant species (Pitchers et al. 2013, Klepsatel et al. 2014).

Although numerous studies have quantified intraspecific morphology across latitude and elevation gradients in insects, those incorporating population genetic data on gene flow and population structure are more limited (but see, for example, Arnett and Gotelli 1999, Keller et al. 2013, Slatyer et al. 2019). Species demography and population genetic structure could relate to adaptive trait evolution along spatial gradients if better dispersal and greater gene flow reduces the potential for local adaptation or drift, while some degree of dispersal restriction could promote morphological divergence with spatial-environmental factors (Kawecki and Ebert 2004, Slatyer et al. 2019). Linking trait variation across populations with underlying population genetic structure should provide additional insights into the possible forces maintaining phenotypic diversity beyond morphological measurements alone (Keller et al. 2013).

Bumble bees (Hymenoptera: Apidae: *Bombus* spp.) provide an interesting group for investigating body size clines. These eusocial insects (Goulson 2010) possess numerous traits that make them especially well suited to life at lower temperatures (Heinrich 2004), including large body size, dense pile, and a capacity to generate heat by shivering thoracic muscles at low ambient temperatures (Heinrich and Kammer 1973; Heinrich 1975, 1976, 1977; Peat et al. 2005). Bumble bees also possess traits that facilitate flight and might improve their ability to thrive at high elevations, such as variation in wing loading or ability to alter wingbeat kinematics (Dudley and Ellington 1990, Dillon et al. 2006, Dillon and Dudley 2014). Because of their capacity for facultative endothermy, bumble bees might be expected to exhibit characteristics of body size evolution comparable to other endothermic animals, and thus may be more likely to exhibit Bergmann's clines than other insects. However, as discussed above, large size may pose challenges to flight. Given bumble bee dependence on flight for foraging and dispersal, there may be trade-offs between thermoregulation and flight that could complicate simple relationships between body size and latitude or temperature. Although bees in general seem to follow Bergmann's rule, studies that have investigated clinal variation in size related traits in *Bombus* have produced conflicting results (Dillon et al. 2006, Gérard et al. 2018). Peat et al. (2005) investigated diverse bumble bee species and found that within species, northern populations from cool environment were larger than southern populations; among species, cold-associated species were often larger than species from warmer areas; however, counter to expectations, tropical species from "hot" climates were still larger. Scriven et al. (2016) also identified patterns of size variation consistent with Bergmann clines among species. However, Ramirez-Delgado et al. (2016) used comparative phylogenetics to show a negative size–latitude relationship across species, but only considered mean values for each species and did not take into account intraspecific variation. Thus, while considerable size variation in *Bombus* is common, the mechanisms that shape variation within particular taxa remain unclear and may differ among species.

In this study, we compare patterns of intraspecific trait variation for two bumble bee species, *Bombus vosnesenskii* and *Bombus vancouverensis nearcticus* (Ghisbain et al. 2020), sampled across latitude (36.5–48.6° N) and altitude (49–2,293 m) in the Sierra-Cascade Mountain region of California, Oregon, and Washington, United States (Fig. 1). Both species can be found from sea level to several thousand meters in elevation, but *B. vancouverensis* tends to be restricted to relatively higher elevations throughout this region compared to *B. vosnesenskii*, especially in the southern Sierras. Consistent with its broader elevational distribution in the region, *B. vosnesenskii* is seemingly the more dispersive species, exhibiting much weaker range-wide population genetic structure and significantly larger foraging ranges (Lozier et al. 2011, Jackson et al. 2018, Mola et al. 2020). We analyze multiple traits, including body mass, body size, wing area, and foraging loads, alongside population genetic data (restriction site associated DNA sequences, or RADseq) to create a data set including trait measurements and single nucleotide polymorphisms (SNPs) for hundreds of bees.

We test several expectations regarding the influence of latitude, elevation, and annual mean temperature (AMT) on morphological traits. If Bergmann's rule applies to bumble bees, body size should increase with latitude and/or elevation. If heat conservation is the primary mechanism driving Bergmann clines, body mass should be negatively correlated with AMT. Deviations from these predictions would suggest alternative mechanisms underlying intraspecific trait variation. One alternative mechanism is that thinner air at

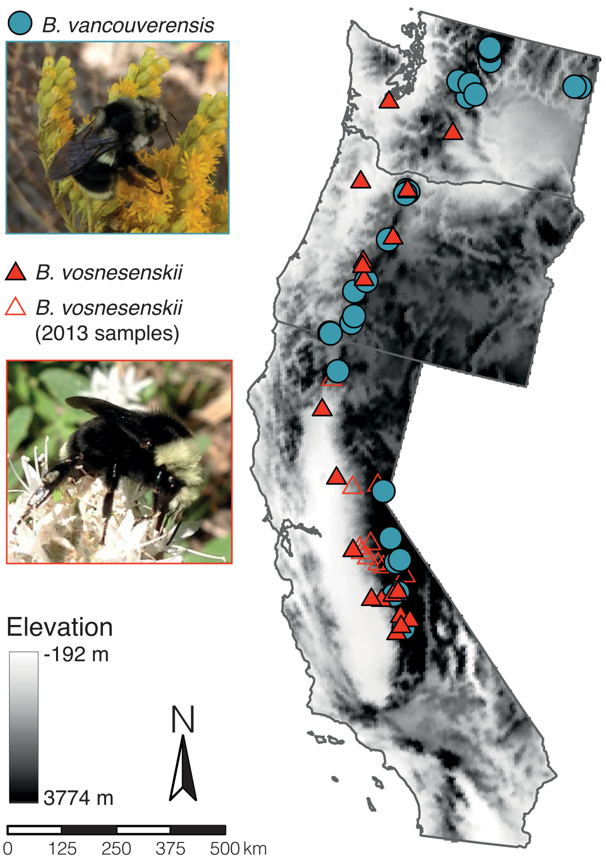

Fig. 1. Map of sampling localities in California, Oregon, and Washington, United States. *Bombus vancouverensis* is indicated by circles, *B. vosnesenskii* by triangles, and additional *B. vosnesenskii* from 2013 used to improve elevational coverage at middle latitudes for some traits by open triangles. Grayscale shading reflects a digital elevation model for the region.

high altitudes select for smaller body sizes, which would be evident through reduced wing loading. Population genetic structure may also influence clinal variation in morphological traits, as the amount of gene flow in bee populations is related to body size variation (López-Uribe et al. 2019). Because *B. vancouverensis* populations are restricted to high elevations in parts of the species range and exhibits reduced gene flow (Jackson et al. 2018, 2020), this species may be particularly likely to exhibit adaptive morphological variation, especially related to flight.

Materials and Methods

Sampling, Morphological Measurement, and Site Characterization

Worker bee specimens were obtained for *B. vancouverensis* (all belonging to the black-banded *nearcticus* lineage) and *B. vosnesenskii* workers from California, Oregon, and Washington, United States (see Jackson et al. 2018, 2020) (Fig. 1). In the field, we measured the mass of worker bees and their foraging loads carried at time of collection by first weighing bees (incapacitated by chilling on ice) as collected ('field mass', with pollen balls and full nectar load). We then determined an 'empty mass', where we removed pollen balls and emptied the honey stomach by pressing the underside of the abdomen to force complete nectar regurgitation. We did not collect empty mass data for every bee in the study (only field mass was measured in 2014). Analyses of field mass therefore include slightly more samples. Foraging load was estimated by subtracting empty mass from field mass. For this study, we retained specimens that were collected during the same time period (2014–2016), and which had genetic data for at least four specimens per sample site from our prior study (Jackson et al. 2018, 2020). This resulted in a data set with 347 bees from 34 localities for *B. vancouverensis* and 242 bees from 20 localities for *B. vosnesenskii* (but see Results for details on analyses repeated to include additional *B. vosnesenskii* samples from 2013; Fig. 1). Based on relatedness estimates from a prior genetics study (Jackson et al. 2018), each bee in this data set comes from a separate colony.

Wing area was measured from wings clipped at the wing base and mounted with fore- and hindwing separated to microscope slides with transparent tape. We mounted both sets of fore- and hindwings for most bees, but because wing damage is common in older bumble bees (Foster and Cartar 2011), we selected the most intact ipsilateral fore- and hindwing for imaging (if both wing sets were damaged, we excluded the sample). To determine area, slide mounted wings were scanned on a flatbed scanner (Epson V30 Perfection, 1,200 dpi) with a 1-mm microscope calibration slide (Zeiss). The calibration slide was used to determine the scaling factor (pixels/mm) for subsequent analyses. Wing images were loaded into Gimp 2.8.22 (www.gimp.org) and cut out from the background using the Scissor select tool's intelligent edge fitting. The digitally cut out wings were made completely white and pasted onto a black background. These binary images were then loaded into imageJ (Schneider et al. 2012) to calculate the area of each wing in mm^2 using the predetermined scaling factor. Wing loading (p_w) in units of N/m^2 was determined from wing area and field mass ($p_{w\text{-Field}}$) or empty mass ($p_{w\text{-Empty}}$) measurements using the equation p_w = (m*g)/(2S), where m = field or empty mass of the bee (in kg) and S = area (in m^2) from the one measured set of wings, g = the gravity constant (9.8 m/s).

We also measured the intertegular span (ITS) of the thorax of each bee, a commonly used measure of size in bees that correlates with body mass (Cane 1987, Hagen and Dupont 2013, Kendall et al. 2019) and is independent of loading state (i.e., whether the animal has a full crop; Vogt and Dillon 2013). Bees were held in place such that the dorsal thorax of each specimen could be held in focus, photographed, and digitally calibrated using a Leica M165c digital stereo microscope (Wetzlar, Germany). In ImageJ, we first determined scaling for each image by measuring the length (in pixels) of the embedded 5-mm digital calibration scale bar. ITS was determined by measuring the distance between the outermost edges of the tegula in pixels and converting back to millimeters using the known scaling factor.

Coordinates and elevation for each collection site were taken using a handheld Garmin eTrex 30× GPS unit. We used the R 3.6.2 (R Core Team 2019) package raster v3.0-12 (Hijmans 2020) to extract AMT for each site (BIO1 from the WorldClim data set) (Hijmans et al. 2005) (Supp Fig. S1 [online only]). AMT is highly correlated with most other temperature variables across our study sites (e.g., correlation with BIO10, the mean temperature of the warmest quarter, is r = 0.98 for this region) and is strongly predictive of thermal tolerance in bumble bees (Pimsler et al. 2020). We thus expect this variable to capture the temperature variation relevant for large-scale Bergmann clines. Latitude, elevation, and AMT were centered and scaled (default scale function in R) whenever statistical models included multiple predictor effects, although some plots show models without scaling (scaling is indicated as needed in tables and figures).

Statistical Analyses

Pearson correlations among traits were determined with the cor.test() function in R and visualized with the psych 1.9.12.31 package (Revelle 2019). For most statistical tests, we performed linear mixed effects regression (lmer) models (Harrison et al. 2018a) with the R package lme4 1.1-21 (Bates et al. 2015) (lmer function), with *P*-values assigned using the Satterthwaite's df estimation method in lmerTest 3.1-1 (Kuznetsova et al. 2017). In the Results section, presented statistics from lmer models include the lmerTest *t* statistic, Satterthwaite's df, and *P*-value for the fixed effect; full model tables are presented in Supp Information (online only). Tables and figures were prepared with sjPlot 2.8.2 (Lüdecke 2020) and ggplot2 3.3.0 (Wickham 2016). Following previous work on size–mass relationships in bees (Hagen and Dupont 2013, Kendall et al. 2019) and examination of model residuals, we employed log transformations of metrics involving ITS and field/empty masses (ITS, masses, and wing loadings) in lmer models. For comparisons of traits between species, lmer models used species as a fixed effect and sampling site as a random effect to account for local site effects. Because of potential collinearity among variables, when evaluating spatial-environmental predictors of trait variation, we first analyzed each fixed effect (elevation, latitude, AMT) in a separate lmer model for each species and trait, with sampling site as a random effect.

Although there are obvious correlations between environmental factors and their influence on traits (see the univariate models in Results and Discussion), we were nonetheless interested in evaluating the combined effects of elevation and AMT on morphological variation in a single model. We a priori expect latitude body size clines to be driven by temperature under Bergmann's rule, and we thus do not consider the spatial variable latitude in these models; however, latitude and longitude were included as random effects using spatial mixed effect modeling. We fit spatial models with the fitme function in the R package spaMM (Rousset and Ferdy 2014). Fixed effects were specified as above, but geographic coordinates were used directly as random effects with a Matérn correlation matrix term and models were fit with a gamma family distribution and log-link. We tabulated Akaike information criterion (AIC) for all models derived from the starting models for each species:

$$\begin{aligned} \text{f itme } [(\text{mass},\ p_w,\ \text{or ITS}) &\sim \text{scale}(\text{AMT}) + \text{scale}(\text{elevation}) \\ &+ \text{scale}(\text{AMT}) * \text{scale}(\text{elevation}) \ + \ \text{Matern}(1|x+y)] \end{aligned}$$

The lowest AIC model was retained as the final model and we used the confint function to generate 95% confidence intervals (CIs) for each fixed effect estimate.

For foraging load, which had numerous zero measurements and required transformation to improve normality of residuals, we performed generalized linear mixed models (GLMMs) in the package glmmTMB (Brooks et al. 2017) using a zero-inflation model and a ziGamma distribution with a log-link. We also performed an alternative lmer analysis of log-transformed foraging load that excluded zero values, but results were qualitatively similar to the zero-inflated models (not shown). We used MuMIn v1.43.15 (Bartoń 2019) to automatically calculate AIC for the GLMM models and present the final model as that with lowest AIC (setting REML = FALSE in lme4 to use maximum likelihood for model comparisons).

Integrating Morphological and Population Genetic Dissimilarities

We also tested the relationship of morphological clines with patterns of population genetic structure estimated using SNP data from prior RADseq work (Jackson et al. 2018). We used VCFtools (Danecek et al. 2011) to filter raw SNP calls (which had a minimum sequencing depth of 5× and genotype quality score of 10, and <15% missing data). Because *B. vancouverensis* had a larger number of total SNPs, to make the data sets comparable, we randomly selected 10,000 of the resulting biallelic SNPs with a minor allele frequency of 5% from each species. Matrices used for analyses included pairwise trait differences, genetic structure (pairwise F_{ST}), elevation differences, pairwise distances for AMT, and spatial distance calculated between each population pair. We calculated mean and pairwise F_{ST} (Weir and Cockerham method) for each pair of localities within each species using hierfstat (Goudet and Jombart 2018). For morphological traits, we focused on field mass and $p_{w\text{-Field}}$ to maximize the number of populations that could be included, given similarity in relative patterns for field and empty values when both mass measurements were available. We calculated the pairwise Euclidean distance between population means for each trait and the associated site elevation and AMT (population means rescaled using the R scale function) using ecodist 2.0.3 (Goslee and Urban 2007). Finally, we calculated pairwise geographic distance (km) with distm (distGeo option) in the R package geosphere 1.5-10 (Hijmans 2019).

To test main effects of space, elevation, and genetic structure on morphological traits, we used two approaches: Maximum Likelihood Population Effects (MLPEs) modeling (Clarke et al. 2002) and Multiple Regression on Distance Matrices (MRMs) (Legendre et al. 1994). MLPE was conducted using mlpe_rga in the package ResistanceGA 4.0-14 (Peterman et al. 2014, Peterman 2018), which is a linear mixed model approach that factors in multiple pairwise comparisons using population as a random effect. MRM and significance testing were conducted with default settings in ecodist. We examined models testing the effects of the various distance matrixes on morphological dissimilarity for each method. MLPE models were compared with AIC.

Results

General Trait Characteristics Within and Between Species

Worker bees of both species varied considerably in size metrics both within and between sites across their geographic ranges (Figs. 2 and 3; Supp Table S1 [online only]). Traits were highly correlated within individuals for each species (Supp Fig. S2 [online only]), including, for example, mass and wing area (e.g., Pearson's correlations for empty mass and forewing area: *B. vancouverensis* $r = 0.83$, $t = 24.3$, df = 272, $P < 0.001$; *B. vosnesenskii* $r = 0.86$, $t = 24.3$, df = 204, $P < 0.001$), and forewing and hindwing area (*B. vancouverensis* $r = 0.93$, $t = 46.97$, df = 345, $P < 0.001$; *B. vosnesenskii* $r = 0.97$, $t = 61.6$, df = 240, $P < 0.001$). Between the two species, lmer models showed that *B. vosnesenskii* workers were significantly larger than *B. vancouverensis*, with greater mass (field: $t = 10.2$, df = 64.7, $P < 0.001$; empty: $t = 9.8$, df = 58.8, $P < 0.001$; Fig. 2A and B), ITS

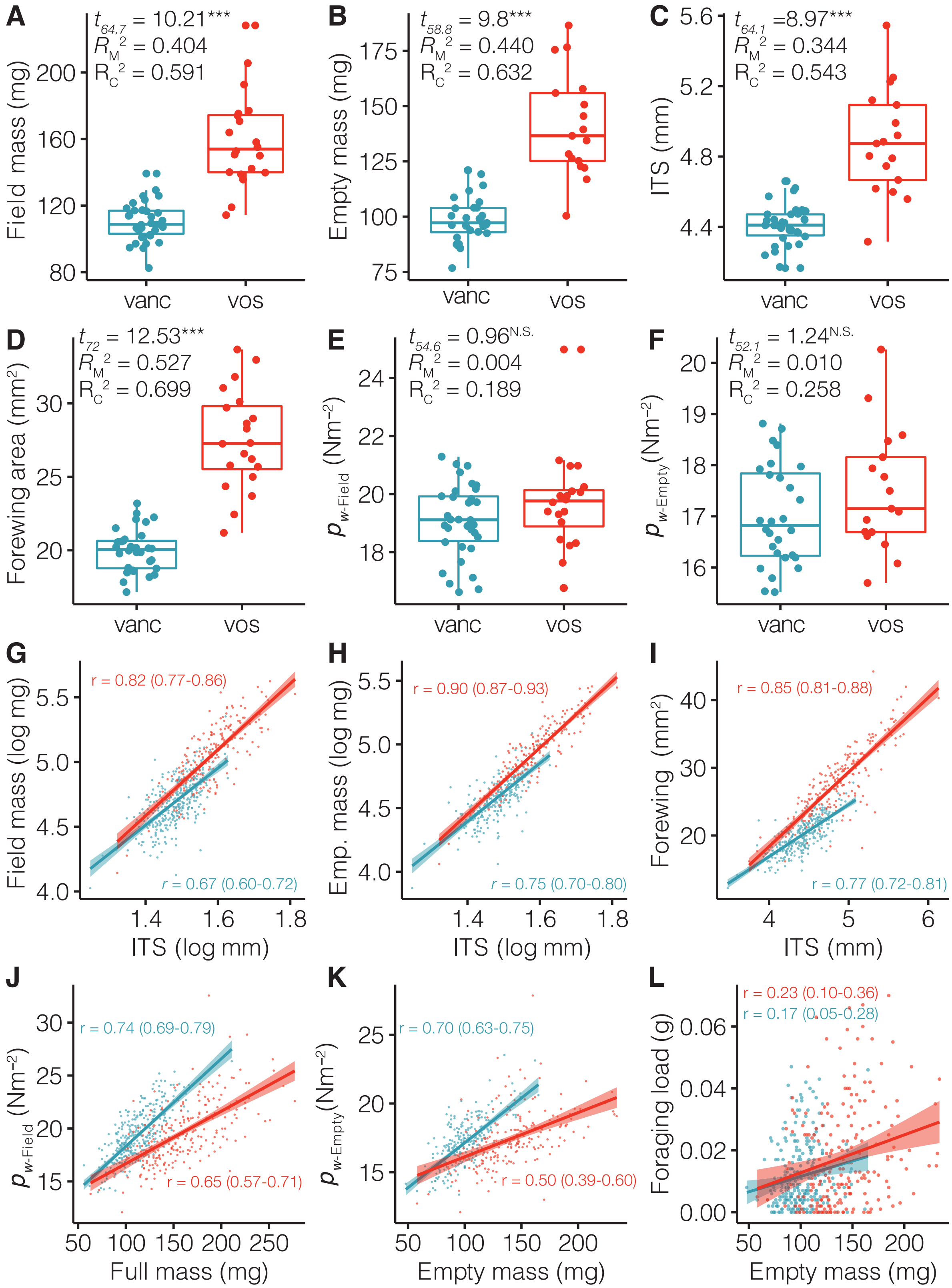

Fig. 2. Boxplots (shown for site means) and tests of differences between species in overall field mass (A), empty mass (B), ITS (C), forewing area (D), $p_{w\text{-Field}}$ (E), and $p_{w\text{-Empty}}$ (F). Statistical tests are summaries taken from linear mixed models (full report and parameter estimates in Supp Table S1 [online only]), showing marginal (R_M^2) and conditional (R_C^2) R^2 values and with df for the species effect *t* statistic and *P*-values (****P* < 0.001; N.S. = not significant) associated with the relevant fixed effect estimated using lmertest. Mass, ITS, and *pw* values were log-transformed for statistical tests but plotted untransformed. Panels G–L show scatterplots of correlations among several traits for each bee and are presented with Pearson's correlation coefficients (*r*) and 95% CIs (see Supp Tables 2 and 3 [online only] and Supp Figs. S2–S4 [online only] for additional trait correlation statistical details).

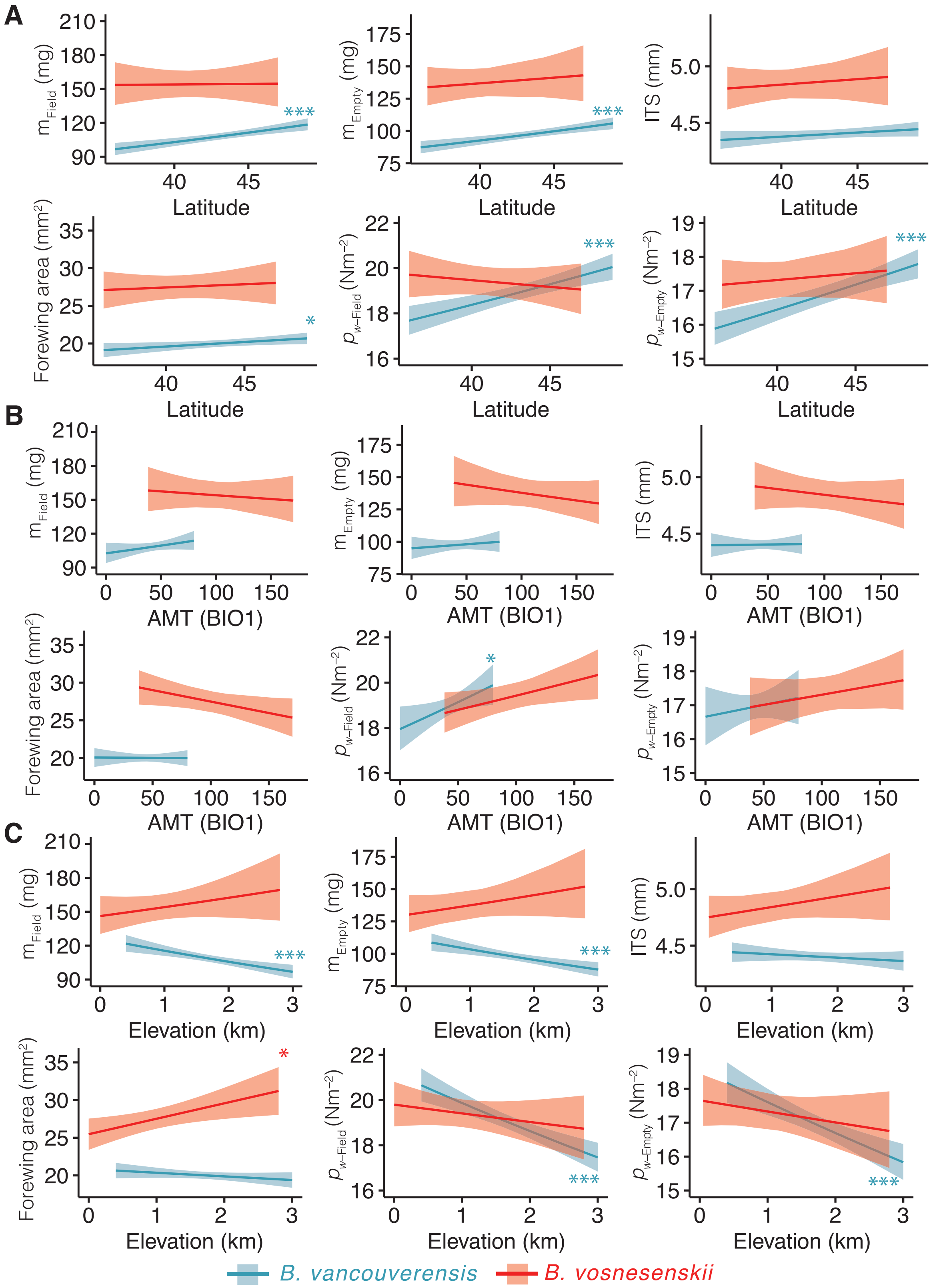

Fig. 3. Effect predictions (with 95% CI) of mass (field and empty), thorax size (ITS), forewing area, and transformed wing loading ($p_{w\text{-}Field}$, $p_{w\text{-}Empty}$) against (A) latitude, (B) AMT (Worldclim BIO1 variable), and (C) elevation from univariate linear mixed effects models for *B. vancouverensis* (blue) and *B. vosnesenskii* (red). Statistical analyses were conducted on log-transformed mass, ITS, and wing loading (see Supp Table S4 [online only]), but responses were back-transformed to the original scale for plotting (plot_model function in sjPlot). Lines are labeled with significance estimate of the β parameter estimated from lmerTest (*$P < 0.05$; ***$P < 0.001$; unlabeled = not significant, CI encompasses zero).

(t = 8.98, df = 64.1, P < 0.001; Fig. 2C), and forewing area (t = 12.5, df = 71.99, P < 0.001; Fig. 2D) (Supp Table S2 [online only]). Foraging loads at the time of sampling were also larger in *B. vosnesenskii* (17.8 mg ± 1.14 SE mg per bee) than *B. vancouverensis* (11.5 ± 0.63 SE mg per bee), but differences could largely be explained by size differences between the species (i.e., larger bees carried significantly larger loads), with no significant species effect when mass was included in the GLMM (Table 1; Fig. 2L). The lmer models identified a significant association between log-transformed ITS and mass (field or empty) (Fig. 2G and H); however, there was also a species effect, with *B. vosnesenskii* being significantly heavier for a given thorax size (Supp Table S2 [online only]). There were no significant differences between the species in mean wing loading ($p_{w\text{-Field}}$: t = 1.0, P = 0.33; $p_{w\text{-Empty}}$: t = 1.2, P = 0.22), although there were clear differences between species in the correlation between p_w and mass for the species (Fig. 2J and K) due to relatively small increases in wing area with body size in *B. vancouverensis* (Fig. 2I; Supp Table S3 [online only]).

Spatial Trait Correlations Within Species

Given prior studies that have investigated the potential for Bergmann's rule to operate within *Bombus* (e.g., Peat et al. 2005, Ramirez-Delgado et al. 2016, Scriven et al. 2016), we first tested the effects of latitude on size traits for each species under the hypothesis that bees should generally be larger at higher latitudes (Fig. 3A; Supp Table S4a and b [online only]). Indeed, for *B. vancouverensis*, we found significant increases with latitude in the lmer models for field mass (t = 4.73, df = 34.07, P < 0.001), empty mass (t = 4.74, df = 27.15, P < 0.001), forewing area (t = 2.16, df = 33.47, P = 0.03), $p_{w\text{-Field}}$ (t = 4.52, df = 33.78, P < 0.001), and $p_{w\text{-Empty}}$ (t = 4.98, df = 27.73, P < 0.001). In *B. vosnesenskii*, no traits were significantly affected by latitude (Fig. 3A; Supp Table S4b [online only]). Despite the clear relationship between ITS and body mass estimates (Fig. 2A and B) and the highly significant latitude–mass and latitude–wing area relationships, we found no significant effect of latitude alone on ITS in either species (Fig. 3A; Supp Table S4a and b [online only]), although trends were in the same direction as for mass (Fig. 3A; Supp Fig. S3 [online only]).

The *B. vancouverensis* mass–latitude effect is consistent with expectations for an intraspecific Bergmann cline; however, when we evaluated the effects of AMT (Fig. 3B; Supp Table S4c and d [online only]), there was no significant association with traits, except for a marginal increase in $p_{w\text{-Field}}$ with AMT (t = 2.24, df = 35.18, P = 0.03). Although not significant, bees tended to be larger at warmer sites for *B. vancouverensis*, which is opposite the direction expected if the observed latitudinal Bergmann's cline was driven by thermoregulation. There were no significant effects of AMT on size traits in *B. vosnesenskii*.

We next considered effects of elevation to test the hypothesis that morphology changes could be associated with flight in thinner air (Fig. 3C; Supp Table S4e and f [online only]). Mass was significantly smaller with elevation for *B. vancouverensis* (field: t = −4.12, df = 33.71, P < 0.001; empty: t = −3.83, df = 26.46, P < 0.001), but not for *B. vosnesenskii* (Fig. 3C; Supp Table S4e and f [online only]). As for latitude, there was no significant effect of elevation on ITS. The distinction of ITS from mass in *B. vancouverensis* could stem from a complex relationship between mass and ITS that changes with elevation; a lmer model evaluating the relationship between ITS and mass that included elevation as a covariate indeed

Table 1. Zero-inflated GLMMs (modeled using a zero-inflated Gamma distribution with log-link in glmmTMB package) examining effects of (a) species and mass on foraging loads (estimated from bee mass difference with removal of pollen and nectar), and the delta-AICc selected models for (b) *B. vancouverensis* and (c) *B. vosnesenskii* species-specific foraging loads

(a)	Foraging load (mg)			
Predictors	Estimate	SE	z	P
Intercept	13.42	0.074	35.003	<0.001
Species (*B. vosnesenskii*)	1.235	0.127	1.667	0.096
Scaled bee empty mass (mg)	1.196	0.061	2.952	0.003
Zero-inflated model				
Intercept	0.096	0.162	−14.514	<0.001
N_{obs}: 480, N_{groups}: 44				
(b)	*B. vancouverensis* foraging load (mg)			
Intercept	12.206	0.061	41.05	<0.001
Scaled AMT (BIO1)	1.122	0.055	2.082	0.037
Scaled bee empty mass (mg)	1.148	0.058	2.395	0.017
Zero-inflated model				
Intercept	0.083	0.227	−10.96	<0.001
N_{obs}: 274, N_{groups}: 28				
(c)	*B. vosnesenskii* foraging load (mg)			
Intercept	18.918	0.064	46.067	<0.001
Scaled bee empty mass (mg)	1.212	0.065	2.934	0.003
Scaled latitude	0.911	0.061	−1.526	0.127
Zero-inflated model				
Intercept	0.114	0.23	−9.449	<0.001
N_{obs}: 206, N_{groups}: 17				

Analyses were repeated using standard lmer with log-transformed foraging loads (excluding all bees with no measured foraging load) and results were identical, with the exception that the top *B. vosnesenskii* model did not include the insignificant latitude effect (not shown).

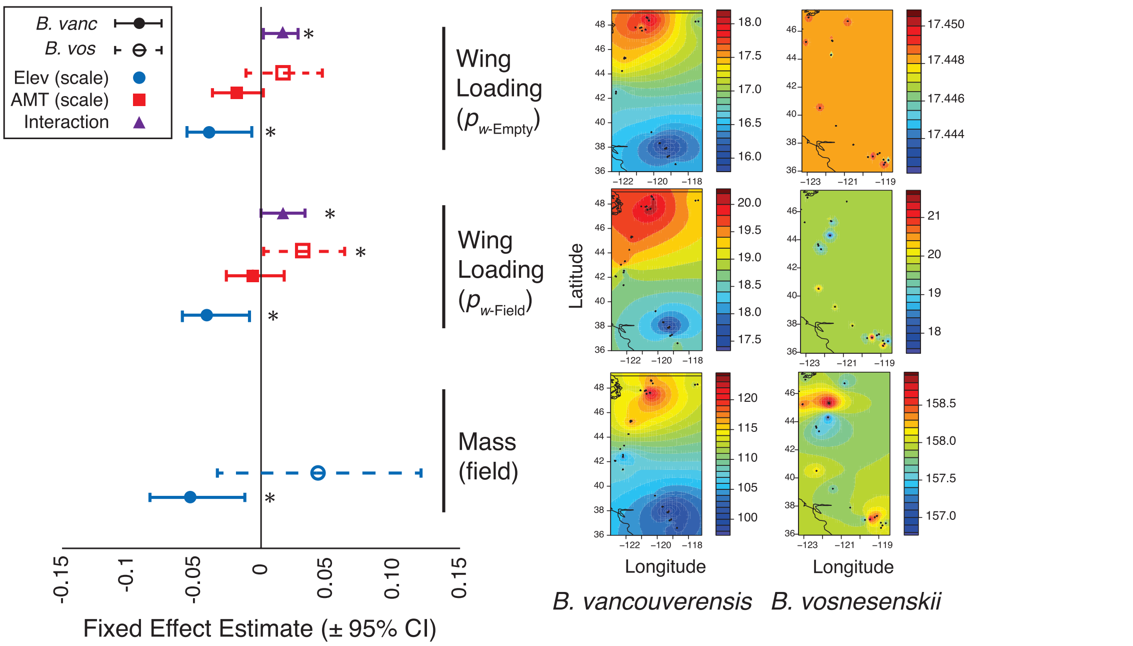

Fig. 4. Parameter estimates for fixed effects (β) in spatial mixed effects models (spaMM) for each species, with 95% CIs, testing the effects of Elevation (scaled), AMT (scaled), and Elevation * AMT interaction on traits; Asterisk indicates the CIs did not encompass zero. If no estimate is shown that variable was not included in the model for that species. Maps show spatial trends of trait value from interpolation of estimates for each model (filled.mapMM function in spaMM). Note, for *B. vosnesenskii* mass and $p_{w\text{-Empty}}$, the low-AIC models were intercept plus random effect only, but for visualization, results are presented for the next best model with at least one fixed effect (see Table 2 for model details).

suggests an interaction effect, where *B. vancouverensis* workers are lighter at high elevations relative to their ITS (Supp Fig. S4 [online only]). Such an effect was absent in *B. vosnesenskii*, with ITS being the sole best predictor of mass (Supp Fig. S4 [online only]). Consistent with the predicted impact from challenges to flight at elevation, *B. vancouverensis* showed clear and significant reductions in p_w with elevation ($p_{w\text{-Field}}$: $t = -5.15$, df = 35.07, $P < 0.001$; $p_{w\text{-Empty}}$: $t = -4.66$, df = 27.40, $P < 0.001$) (Fig. 3C; Supp Table S1e [online only]). For *B. vosnesenskii*, there was no relationship for p_w with elevation (Supp Table S1f [online only]). There was a marginally significant increase in forewing area with elevation in *B. vosnesenskii* ($t = 2.51$, df = 17.84, $P < 0.05$; Supp Table S1f [online only]) but not *B. vancouverensis* (Supp Table S4e [online only]).

The spaMM models considering both elevation and AMT were generally consistent with the results above, suggesting much stronger spatial patterns in *B. vancouverensis* and with a strong reduction in mass and wing loading where the species is restricted to the highest elevations in the south (Fig. 4). For mass, the low-AIC model for *B. vancouverensis* included only a significantly negative elevation effect (95% CI: −0.084 to −0.013), while for *B. vosnesenskii*, the best model only retained the intercept (Table 2 [a]; Supp Table S5 [online only]). For $p_{w\text{-Empty}}$ in *B. vancouverensis*, the complete model (AMT, elevation, interaction) had the lowest AIC; for $p_{w\text{-Field}}$ the complete model and an elevation-only model were essentially tied for AIC; however, we elected to present the complete model because the interaction term CI suggested it was significant (Table 2 [b]; Supp Table S5 [online only]). The *B. vancouverensis* $p_{w\text{-Field}}$ and $p_{w\text{-Empty}}$ models both revealed a significant reduction in wing loading with elevation (95% CIs: −0.060 to −0.009; −0.056 to −0.008), as well as positive elevation–AMT interactions (95% CIs: 0.0002–0.032; 0.0008–0.028) (Table 2 [b and c]). Wing loading in *B. vancouverensis* thus decreased more strongly with elevation at colder AMTs (see also Supp Fig. S5 [online only]). The selected $p_{w\text{-Field}}$ model for *B. vosnesenskii* included an AMT effect (95% CI: 0.002–0.06), while for $p_{w\text{-Empty}}$, an intercept-only model was retained (Table 2 [b]). Top models for ITS in both species only included an intercept, but trends were similar to mass (Supp Fig. S3 [online only]). It is again important to stress that the correlations of spatial variables (Supp Fig. S1 [online only]) make purely statistical conclusions from these observation data challenging, but together with univariate analyses, results suggest that temperature, latitude, and elevation may all influence body size traits in some way for both species, and the effects of these variables on traits differ between the species.

Finally, because we initially restricted our analyses to samples from 2014 to 2016 to standardize sampling periods for the two species, this resulted in fewer sites and samples for *B. vosnesenskii* compared to *B. vancouverensis*, especially for higher elevation sites at intermediate latitudes. We elected to repeat the morphological analyses above by including an additional 159 *B. vosnesenskii* specimens collected from 13 sites in 2013 to evaluate whether the above results could be a result of reduced statistical power (open triangles in Fig. 1). However, repeated analyses detected no additional significant effects and final models were essentially the same as those presented above. The only exceptions were that the marginal elevation effect on forewing area and the AMT effect on $p_{w\text{-Field}}$ were actually not observed in the larger data set. Thus, differences between the species do not appear to be a simple artifact of sampling (detailed in Supp Tables S6–S8 [online only]).

The Phylogeography of Trait Dissimilarity

We investigated the relationship of morphological differences among populations with population structure, distance, and elevation by performing analyses on dissimilarity between sites for body mass and p_w, traits for which we had the most complete data sets. We investigated effects of pairwise spatial distance, which in

Table 2. Results for the final (low AIC; Supp Table S5 [online only]) spaMM spatial mixed models (Gamma family with log-link) for (a) field mass and (b) wing loadings $p_{w\text{-Field}}$ and (c) $p_{w\text{-Empty}}$ (empty mass results were essentially the same as field mass; ITS was also tested but returned intercept-only models for both species; see Supp Fig. S3 [online only])

(a)	*B. vancouverensis* field mass (mg)				*B. vosnesenskii* field mass (mg)			
Predictors	Estimate	SE	t	95% CI (low, high)	Est.	SE	t	95% CI (low, high)
Intercept	4.700	0.016	289.5		5.044	0.037	134.4	
Scaled elevation (km)	−0.053	0.014	−3.51	**−0.084, −0.013**				
Random effects								
ν, ρ	0.257, 5.138				3.22, 37.86			
Random effect variance λ	0.0038				0.023			
Residual variance Φ	0.027				0.035			
N_{obs}, N_{groups}	347, 33				242, 20			
(b)	*B. vancouverensis* $p_{w\text{-Field}}$ (N/m²)				*B. vosnesenskii* $p_{w\text{-Field}}$ (N/m²)			
Intercept	2.961	0.009	326.0		2.971	0.015	203.53	
Scaled AMT (BIO1)	−0.006	0.009	−0.61	−0.026, 0.017	0.03	0.015	2.248	**0.002, 0.064**
Scaled elevation (km)	−0.040	0.009	−4.39	**−0.060, −0.008**				
Scaled AMT * Scaled elevation	0.016	0.007	2.20	**0.0002, 0.0320**				
Random effects								
ν, ρ	0.075, 4.68				2.08, 37.86			
Random effect variance λ	0.001				0.003			
Residual variance φ	0.011				0.018			
N_{obs}, N_{groups}	347, 33				242, 20			
(c)	*B. vancouverensis* $p_{w\text{-Empty}}$ (N/m²)				*B. vosnesenskii* $p_{w\text{-Empty}}$ (N/m²)			
Intercept	2.843	0.008	351.38		2.858	0.015	195.7	
Scaled AMT (BIO1)	−0.019	0.007	−2.60	−0.037, 0.002				
Scaled elevation (km)	−0.040	0.008	−5.07	**−0.056, −0.008**				
Scaled AMT * Scaled elevation	0.015	0.006	2.69	**0.0008, 0.0275**				
Random effects								
ν, ρ	0.065, 0.956				0.005, 32.18			
Random effect variance λ	0.001				0.002			
Residual variance Φ	0.006				0.010			
N_{obs}, N_{groups}	274, 27				206, 17			

Full model fixed effects were latitude, AMT (BIO1) (both center-scaled), and the interaction, with coordinates specified as a random effect using a Matérn correlation matrix (described by correlation smoothness parameter ν and the scale parameter ρ).

this system largely reflects latitudinal separation (Jackson et al. 2018), and elevation. AMT distance matrices did not have a significant effect in any MRM or improve AIC in MLPE models for either species, so are not discussed further. The standardized 10,000 SNP data sets provided highly precise estimates of population structure; F_{ST} values were nearly identical to those previously reported in a larger study (Jackson et al. 2018), with both species weakly structured but *B. vancouverensis* exhibiting nearly sevenfold greater differentiation (F_{ST} = 0.022, 95% CI: 0.021–0.023) than *B. vosnesenskii* (F_{ST} = 0.003, 95% CI: 0.003–0.004). Isolation by distance was also stronger in *B. vancouverensis* (Fig. 5; MRM R^2 = 0.90, $P \leq 0.001$ for *B. vancouverensis*; R^2 =0.10, $P \leq 0.001$ for *B. vosnesenskii*).

Morphological trait variation was correlated with this population structure, especially in *B. vancouverensis* (Fig. 5; Supp Fig. S6 [online only]). In *B. vancouverensis*, dissimilarity among populations for mass and p_w showed clear relationships with F_{ST}, geographic distance and elevation in univariate models (Table 3; Supp Fig. S6a [online only]). Differences in mass for *B. vancouverensis* were largely correlated with genetic differentiation; MLPE models incorporating F_{ST} had the lowest AIC values (ΔAIC > 15.5 compared to any model without F_{ST}), with the F_{ST}-only model having the lowest AIC (Fig. 5A; Table 3) and F_{ST} was significant for all MRM mass models that included population structure alone or in combination with other variables, which also had much larger R^2 values. Geographic distance was significant alone or in combination with elevational distance, but elevational distance was only significant in its univariate MRM and not in combination with other factors (Table 3). For p_w, elevation was significant and produced higher R^2 values whenever included in MRM models in *B. vancouverensis* (Fig. 5A; Supp Fig. S6a [online only]) and all the best performing MLPE models incorporated elevation (ΔAIC > 40.5 vs models excluding elevation). The low-AIC model included elevation and F_{ST}, which was better supported than a model including F_{ST} alone

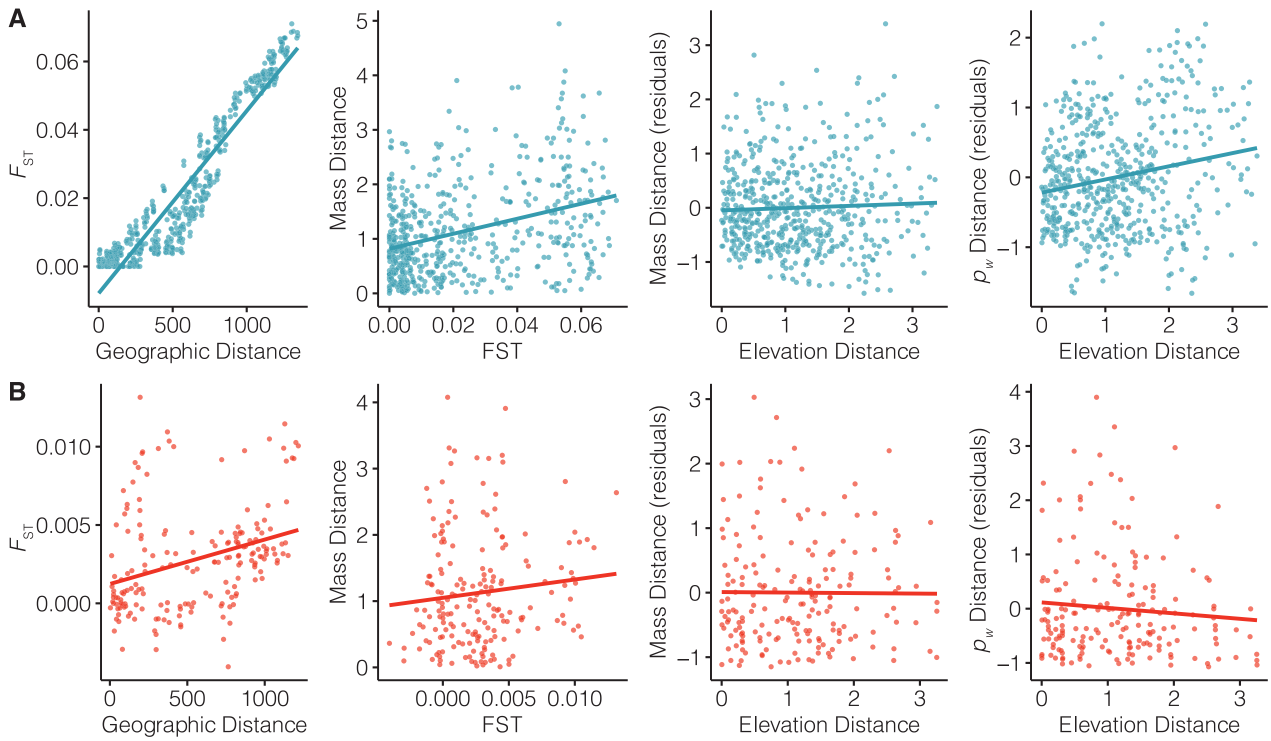

Fig. 5. Relationships among space, population structure (F_{ST}), and average mass and wing loading (p_w) differences among pair of populations for (A) *B. vancouverensis* and (B) *B. vosnesenskii*. Panels include plots of isolation by distance (F_{ST} by geographic distance), effects of population structure on mass, and the effects of elevation on mass and p_w residuals from models including F_{ST} and geographic distance. The latter panels are included to illustrate the remaining positive effect of elevational separation on wing loading differences among *B. vancouverensis* populations after accounting for space and population structure, but not for *B. vosnesenskii* populations and not for mass in either species (see Table 3 and Supp Fig. S6 [online only]).

(ΔAIC = 42.5), but only marginally better than a model with elevation alone (ΔAIC < 2).

For *B. vosnesenskii*, no MRM model explained a particularly large proportion of mass variation and no MLPE model was as strongly favored over the others as in *B. vancouverensis*, although the F_{ST}-only model had the lowest AIC; no models provided compelling explanations of p_w variation (Fig. 5B; Table 3; Supp Fig. S6b [online only]).

Discussion

Body size, mass, and wing dimensions are key traits that may relate to thermoregulatory and flight performance in bumble bees (Heinrich 1977, Dudley 2000, Dillon et al. 2006, Mountcastle et al. 2016). Our results indicate that bumble bees show substantial intra- and interspecific variation in such traits and exhibit complex associations with different spatial-environmental components of species ranges. However, results also suggest that factors shaping morphological attributes are species dependent. *Bombus vosnesenskii* is highly variable in traits but these traits show little correlation with space or AMT, while *B. vancouverensis* shows strong reductions in mass and wing loading at southern high-elevation sites. Uncovering the specific variables driving selection for spatial-environmental correlations will require more work. However, our results suggest that general biogeographic rules (e.g., Bergmann's rule) may not consistently drive evolution of trait dimensions across bumble bees, which could explain some of the conflicting patterns observed in other studies of biogeographic clines (Peat et al. 2005, Scriven et al. 2016, Gérard et al. 2018). Further, we find that reduced gene flow is related to the degree of intraspecific morphological divergence, with clearer signatures of spatial-environmental correlations for traits in the species that likewise has greater spatial population genetic structure, *B. vancouverensis*. This suggests that the same landscapes that produce strong genetic structure may also impact morphology, such that population genetics may be useful for predicting when species are likely to exhibit significant biogeographic variation in functional traits.

Does Bergmann's Rule Apply to *B. vosnesenskii* and *B. vancouverensis*?

The general expectation for Bergmann's rule in endothermic species is that body size should increase with latitude from selection to minimize heat loss at cooler temperatures (Ashton 2002). The first hypotheses we tested were thus a) whether montane bumble bee species followed Bergmann's rule by exhibiting increased body size with latitude and/or elevation and b) whether this would indicate a role for thermoregulation in body size evolution by exhibiting negative correlations with AMT. In *B. vancouverensis*, there was a clear and significant positive correlation of mass and wing size with latitude. However, mass declined with elevation and there was no significant relationship between mass and AMT, both contrasting with expectations for a temperature-driven Bergmann cline. Spatial or environmental associations for bees at different sites were weak or absent for measured traits within *B. vosnesenskii*. Sample sizes were smaller for *B. vosnesenskii* in the main analyses, but this was not likely the cause of comparatively small effects of spatial-environmental variables on trait variation (Supp Tables S6–S8 [online only]). Altogether, results

Table 3. Dissimilarity modeling of pairwise differences in mean wing loading (a) and mass (b) between each population, incorporating genetic distances (F_{ST}) from 10,000 SNPs (0.05 minor allele frequency), pairwise Euclidean differences in elevation (Elev) and pairwise geographic (Geo) distances

(a) $p_{w\text{-Field}}$ distance	*B. vancouverensis*					*B. vosnesenskii*				
	F_{ST}	Elevation distance	Geographic distance	MRM R^2	MLPE AIC	F_{ST}	Elevation distance	Geographic distance	MRM R^2	MLPE AIC
F_{ST}+Elev+Geo	2.366	0.358**	0.000	0.166***	1070.158	−7.52	−0.103	0	0.009	310.5
F_{ST}+Elev	**2.998**	**0.358*****	–	**0.166*****	**1068.182**	−9.28	−0.1	–	0.008	309.7
Elev+Geo	–	0.363***	0.000	0.166***	1068.717	NA	−0.1	0	0.008	310.9
F_{ST}+Geo	8.670	–	0.000	0.102***	1111.455	−3.12	–	0	0.001	309.2
F_{ST}	12.18***	–	–	0.101***	1110.667	**−5.2**	–	–	**0.003**	**308.3**
Elev	–	0.413***	–	0.163***	1069.967	–	−0.1	–	0.007	309.2
Geo	–	–	0.001***	0.097***	1113.628	–	–	0	0.001	309.4
(b) Mass distance										
F_{ST}+Elev+Geo	19.17*	0.079	0.000	0.127**	974.746	26.2	−0.001	0	0.01	389.7
F_{ST}+Elev	11.975**	0.070	NA	0.123**	973.141	27.3	−0.007	–	0.01	387.8
Elev+Geo	–	0.123	0.001*	0.104***	991.478	NA	−0.02	0.0001	0.003	387.9
F_{ST}+Geo	20.56**	–	0.000	0.124***	972.747	26.5	–	0	0.01	387.8
F_{ST}	**13.770*****	–	–	**0.120*****	**971.146**	**27.6**	–	–	**0.01**	**385.9**
Elev	–	0.288***	–	0.074***	1036.802	–	−0.02	–	0.001	386.1
Geo	–	–	0.001***	0.096***	990.286	–	–	0	0.002	386

Each row represents the main predictors included in the model, with the F_{ST}, elevation dist., and geo dist. columns representing estimates from matrix regression models (MRMs) with the overall MRM R^2. AICs were calculated from MLPE models incorporating population as a random effect. The top model values (ΔAIC = 0) are in bold.

Significance for MRM estimates from permutation tests are indicated by *$P < 0.05$, **$P < 0.01$, ***$P < 0.001$.

suggest that the standard thermoregulation-driven Bergmann's rule is unlikely to be a universal explanation for intraspecific body size variation in bumble bees. Given that the larger-bodied *B. vosnesenskii* also tends to occupy warmer sites on average than *B. vancouverensis*, our data are also inconsistent with temperature-driven interspecific body size differences (Fig. 1; Supp Tables S1 and S6 [online only]). Such patterns are consistent with observations that bumble bees of different sizes are not more or less likely to forage at different ambient temperatures (Couvillon et al. 2010a), and suggests that alternative pressures may be more important for the biogeography of body size clines, at least for some species.

Restriction to High Elevations as a Driver of Morphological Clines

A possible explanation for latitude–AMT conflict becomes clear when examining the relationships of traits with respect to altitude, especially in *B. vancouverensis*. High altitudes are in some ways analogous to high latitudes from a bioclimatic perspective, but these environments may have unique influences on insect biology (Hodkinson 2005, Dillon et al. 2006, Horne et al. 2018, McCulloch and Waters 2018, Shah et al. 2020). Flight performance, in particular, is influenced by reduced air density and can also be impacted by temperature or interactions between low air density and low temperatures (Gilchrist and Huey 2004, Dillon and Frazier 2006). High-elevation specialists may thus be especially likely to exhibit trait variation that could conflict with Bergmann cline expectations (Dillon et al. 2006, Keller et al. 2013). Within *B. vancouverensis*, there was clear signature of declining mass with elevation, which also produced sharp reductions in wing loading at the highest elevations (Fig. 3; Table 2) that should reduce induced power and enhance flight performance in low air densities (Dudley 2000). Intriguingly, this negative p_w–elevation relationship was strongest at colder sites (Fig. 4; Table 2; Supp Fig. S5 [online only]), with the elevation–AMT interaction consistent with the hypothesis that effects of low air density on insect flight performance may be exacerbated by low temperatures (Dillon and Frazier 2006, Frazier et al. 2008).

The species complex to which *B. vancouverensis nearcticus* belongs (together with *Bombus bifarius*) tends to be associated with high-elevation habitats throughout much of the United States (Lozier et al. 2011, 2016; Jackson et al. 2018; Ghisbain et al. 2020). As seen in other montane *Bombus* (Duennes et al. 2012, Hines and Williams 2012, Williams et al. 2018), this drives much of the phylogeographic history of the group, and it is possible that morphology in such specialists is adapted more for high-elevation challenges than those imposed by temperature alone. Interestingly, *B. vancouverensis* showed no increase in wing area with elevation and p_w increased faster with mass in *B. vancouverensis* than in *B. vosnesenskii* (and wing area increased more slowly with size; Fig. 2I–K). This contrasts with some other insects, including montane honey bees, in which wing area changes across elevations while body size remains constant (Hepburn et al. 1998, Dillon et al. 2006). This may indicate pressure to reduce body mass for minimizing flight challenges (Gilchrist and Huey 2004) in high-altitude populations of *B. vancouverensis,* while also emphasizing that bees can achieve changes in wing loading through alteration of different traits. In addition to changes in flight morphology, bumble bees at elevation rely on changes in kinematics to fly at altitude (Dillon and Dudley 2014) and appear capable of doing so in a way that minimizes energetic costs (Combes et al. 2020). The smaller body size of high-altitude *B. vancouverensis* may also facilitate oxygen delivery (Vogt and Dillon 2013). Thus, we propose that the latitudinal Bergmann's cline in *B. vancouverensis* is spurious and driven largely by effects of elevation, rather than temperature, on body size. The ability of *B. vancouverensis* to thrive at high altitudes likely reflects a combination of the morphological changes documented here as well as kinematic, thermoregulatory, and respiratory adaptations necessary for survival in these challenging environments, and future physiological studies should aim to investigate the relative importance of such characteristics across the species range.

The integration of population genetic data further supports the stronger morphological clines in *B. vancouverensis* and indicates some possibility that they may be locally adaptive, especially for wing loading. Although morphological differences correlate with genetic differentiation in both species, population structure in *B. vancouverensis* and its relationship with space is clearly stronger than in *B. vosnesenskii* (Table 3; Fig. 5; Lozier et al. 2011; Jackson et al. 2018). *Bombus vancouverensis* is the smaller species, and the greater F_{ST} and isolation by distance are consistent with other studies that show smaller bees are less dispersive (Greenleaf et al. 2007; López-Uribe et al. 2019). The increase in trait dissimilarity with genetic and spatial-environmental differentiation in *B. vancouverensis* (Fig. 5; Table 3) is especially intriguing. Mass was largely correlated with population structure in both species (Fig. 5), while wing loading appeared to be influenced by spatial factors in addition to genetic differentiation alone. Consistent with our hypothesis about the role of selection on flight morphology in high-altitude *B. vancouverensis*, differences in elevation significantly contributed to wing loading differences among populations, even after accounting for F_{ST} and geographic distance (Fig. 5A). Geographic clines in wing loading in other insects have been hypothesized to be adaptive (Norry et al. 2001, Gilchrist and Huey 2004, Dillon et al. 2006, Klepsatel et al. 2014). Our combined genetic and morphology data are consistent with hypotheses of local adaptation to conditions at high elevations as important for shaping intraspecific diversity in montane bumble bees (Jackson et al. 2020). We previously observed comparable molecular signatures of local adaptation in *B. vancouverensis* with genome–environment association analyses (Jackson et al. 2020), and we hypothesize that variation in mass and wing loading is likewise driven by strong selection acting on populations restricted to high elevations of the High Sierras. In contrast, *B. vosnesenskii* is both a better disperser and a greater habitat generalist throughout the region, which may contribute to maintenance of local phenotypic diversity and inhibit any habitat specific adaptive divergence (Horne et al. 2018, Kendall et al. 2019).

Study limitations suggest future directions for understanding adaptation in montane *Bombus*.

There are several limitations to our study that require discussion. First, although spatial-environmental variables are clearly associated with morphological variation, and species differ in the strength of their response to such variables, the strong collinearity in this system poses challenges for unambiguously assigning functional drivers of trait variation (Supp Fig. S1 [online only]). In part, this can be overcome by analyses that focus on AMT and elevation (Fig. 4), as we expect that latitudinal effects on morphology would most commonly be driven by temperature, but nevertheless collinearity is an important and somewhat unavoidable caveat in interpretation of our results. Mechanisms other than temperature can influence latitudinal clines in insects, while mechanisms other than aerodynamics have been proposed for reductions in size with increasing altitude (Chown and Gaston 2010). For example, declines in size with elevation could relate to differences in season length at high-elevation sites, where shorter seasons select for more rapid development and smaller worker size. Prior studies have provided data consistent with season length as a driver of body size clines in *Bombus* (Ramírez-Delgado et al. 2016, Gérard et al. 2018); however, such studies identified converse Bergmann clines with latitude from reduced season length nearer the poles, which we do not see here. Another possibility is that, at high enough altitudes, oxygen limitation during development could limit adult size and allometry of flight morphology (e.g., Frazier et al. 2001, Woods 2004, Harrison et al. 2010). Ultimately, experiments examining thermal tolerance (Oyen et al. 2016, Pimsler et al. 2020), oxygen limitation (Frazier et al. 2001), and flight performance (Dillon and Dudley 2014) in laboratory-reared colonies sampled across spatial and environmental extremes will be needed to fully understand the mechanistic drivers of variation in morphology, a major challenge for bumble bees.

Second, even accounting for genetic differentiation, we cannot unambiguously invoke a role for selection, and future studies would benefit from estimates of heritability in body and wing dimensions to facilitate comparisons of selection and drift (i.e., true Q_{ST}–F_{ST} comparisons) (Whitlock and Guillaume 2009). Developmental temperature-induced plasticity in wing and body size is known in insects (e.g., Gilchrist and Huey 2004, Chown and Gaston 2010, Pesevski and Dworkin 2020), although bumble bee nests tend to be temperature regulated so this effect may be lessened (Heinrich 2004, Scriven et al. 2016). Bumble bee workers do exhibit variation in size even within nests (Couvillon et al. 2010a, b), which can be influenced by factors such as age or nutrition (reviewed in Chole et al. 2019) and may vary over time (but see Couvillon et al. 2010b). Body size clines among populations could thus arise from autocorrelated spatial or temporal clines in floral resource availability or nest provisioning across sampling sites. Even body size clines produced from resource limitation could be adaptive, however, as smaller bees might be more starvation resistant (Couvillon and Dornhaus 2010). Body size and wing dimensions do commonly have a genetic basis in insects (Chown and Gaston 2010, Pitchers et al. 2013, Klepsatel et al. 2014), including bees, that might contribute to local adaptation even if plasticity does play a role (Daly et al. 1991, Hunt et al. 1998, Calfee et al. 2020). The genetic basic of such variation in *Bombus* remains to be determined, but new reference genomes for these species (Heraghty et al. 2020) should facilitate future studies to detect loci contributing to morphology.

As a final point, our data show that reductions in mass are not fully captured by the linear body size metric ITS. When mass is modeled as a function of both ITS and elevation, *B. vancouverensis* individuals tend to be somewhat lighter at high elevations than predicted by their thorax size (Supp Fig. S4 [online only]). This suggests that *B. vancouverensis* may be reducing mass at elevation in a manner not reflected in thoracic size (see also Kelemen et al. 2020). We tested whether bees might manipulate foraging loads to reduce wing loading, but we found little evidence for this. High-elevation *B. vancouverensis* thus appear to be reducing mass through some alternative, yet to be determined, mechanism. One practical implication is that results from proxies like ITS may not fully reflect ecologically relevant body mass measurements within species. ITS can quickly and easily be measured from both field and natural history collection specimens and has routinely been used as a proxy for mass or size in bees (Greenleaf et al. 2007, Hagen and Dupont 2013, Kendall et al. 2019), but accurate measurement of the small differences (< 1–2 mm) among individuals within species can be challenging, and the unreliability of ITS as a predictor of mass within bee species has been recognized (Kendall et al. 2019). Although ITS and mass are correlated, each metric may capture some unique aspects of morphology in certain conditions (Kelemen et al. 2020), and both should be considered where necessary.

Conclusion

In conclusion, both *B. vosnesenskii* and *B. vancouverensis* exhibit morphological variation across their ranges, but only in *B. vancouverensis* does trait variation clearly track spatial and environmental differences among sites. Bergmann's rule is not universal even for bumble bees from similar geographic regions, and where size–latitude clines are apparent, they may not be driven by temperature. Our results show that pressures associated with altitude are likely important drivers of body mass and wing loading reductions in high-elevation specialists like *B. vancouverensis*. One implication is that if evolution drives local trait adaptation in high-elevation specialists like *B. vancouverensis*, more generalist bumble bee species may face challenges as low-elevation sites become increasingly inhospitable and populations are forced to shift upslope (Kerr et al. 2015, Sirois-Delisle and Kerr 2018). Species like *B. vosnesenskii* that are less restricted to high-elevation habitats may not possess the necessary trait adaptations that more specialized species have evolved for dealing with non-thermal challenges. Experimental work to investigate the physiological implications of morphological trait variation for processes like thermoregulation and flight performance across populations and species will be crucial for understanding the ultimate implications of this intra- and interspecific morphological variation.

Supplementary Data

Supplementary data are available at *Insect Systematics and Diversity* online.

Acknowledgments

The National Science Foundation provided funds to JDL, MED, and JS to support research on local adaptation in these species (DEB-1457645/1457659, URoL-1921585/1921562); MED was also supported by NSF OIS-1826834; MLP was supported by United States Department of Agriculture 2018-67012-28040. Any opinions, findings, conclusions, or recommendations presented are those of the author(s) and do not necessarily reflect the views of the National Science Foundation. We thank the National Parks Service for access to Sequoia/Kings Canyon, Yosemite and Olympic National Parks, and various undergraduate researchers who contributed to specimen processing and imaging.

Author Contributions

JDL collected specimens, performed statistical analyses, and wrote the paper. MED assisted with field work, mass measurement techniques, and statistical analyses, and wrote the paper. ZMP and LR measured ITS and wings, performed preliminary statistical analyses, and contributed to the methods text. JMJ collected specimens and performed field mass measurements. MLP and KJO assisted with field work. All authors contributed to editing the paper. JDL, MED, and JS developed the project and obtained funding for the work.

Data Availability

Morphological and genetic data (VCF files) are available on FigShare (doi:10.6084/m9.figshare.14378843).

References Cited

Altshuler, D. L., R. Dudley, and J. A. McGuire. 2004. Resolution of a paradox: hummingbird flight at high elevation does not come without a cost. Proc. Natl Acad. Sci. USA 101: 17731–6.

Angilletta, M. J., T. D. Steury, and M. W. Sears. 2004. Temperature, growth rate, and body size in ectotherms: fitting pieces of a life-history puzzle. Integr. Comp. Biol. 44: 498–509.

Arnett, A. E., and N. J. Gotelli. 1999. Bergmann's rule in the ant lion *Myrmeleon immaculatus* DeGeer (Neuroptera: Myrmeleontidae): geographic variation in body size and heterozygosity. J. Biogeogr. 26: 275–283.

Ashton, K. G. 2001. Are ecological and evolutionary rules being dismissed prematurely? Divers. Distrib. 7: 289–295.

Ashton, K. G. 2002. Patterns of within-species body size variation of birds: strong evidence for Bergmann's rule. Ecology 11: 505–523.

Ashton, K. G., and C. R. Feldman. 2003. Bergmann's rule in nonavian reptiles: turtles follow it, lizards and snakes reverse it. Evolution 57: 1151–1163.

Ashton, K. G., M. C. Tracy, and A. De Queiroz. 2000. Is Bergmann's rule valid for mammals? Am. Nat. 156: 390–415.

Bartoń, K. 2019. MuMIn: multi-model inference. R package version 1.43.15.

Bates, D., M. Mächler, B. Bolker, and S. Walker. 2015. Fitting linear mixed-effects models using lme4. J. Stat. Softw. 67: 1–48.

Bergmann, C. 1847. Über die Verhältnisse der Wärmeökonomie der Thiere zu ihrer Grösse. Göttinger Stud. 3: 595–708.

Blanckenhorn, W. U., and M. Demont. 2004. Bergmann and converse Bergmann latitudinal clines in arthropods: two ends of a continuum? Integr. Comp. Biol. 44: 413–424.

Brooks, M. E., K. Kristensen, K. J. van Benthem, A. Magnusson, C. W. Berg, A. Nielsen, H. J. Skaug, M. Maechler, and B. M. Bolker. 2017. glmmTMB balances speed and flexibility among packages for zero-inflated generalized linear mixed modeling. R J. 9: 378–400.

Calfee, E., M. N. Agra, M. A. Palacio, S. Ramírez, and G. Coop. 2020. Selection and hybridization shaped the rapid spread of African honey bee ancestry in the Americas. PLoS Genet. 16: e1009038.

Cane, J. H. 1987. Estimation of bee size using intertegular span (Apoidea). J. Kansas Entomol. Soc. 60: 145–147.

Chole, H., S. Hollis Woodard, and G. Bloch. 2019. Body size variation in bees: regulation, mechanisms, and relationship to social organization. Curr. Opin. Insect Sci. 35: 77–87.

Chown, S. L., and K. J. Gaston. 2010. Body size variation in insects: a macroecological perspective. Biol. Rev. 85: 139–169.

Clarke, R. T., P. Rothery, and A. F. Raybould. 2002. Confidence limits for regression relationships between distance matrices: estimating gene flow with distance. J. Agric. Biol. Environ. Stat. 7: 361–372.

Combes, S. A., S. F. Gagliardi, C. M. Switzer, and M. E. Dillon. 2020. Kinematic flexibility allows bumblebees to increase energetic efficiency when carrying heavy loads. Sci. Adv. 6: eaay3115.

Couvillon, M. J., and A. Dornhaus. 2010. Small worker bumble bees (*Bombus impatiens*) are hardier against starvation than their larger sisters. Insectes Soc. 57: 193–197.

Couvillon, M. J., G. Fitzpatrick, and A. Dornhaus. 2010a. Ambient air temperature does not predict whether small or large workers forage in bumble bees (*Bombus impatiens*). Psyche A J. Entomol. 2010: 1–8.

Couvillon, M. J., J. M. Jandt, N. Duong, and A. Dornhaus. 2010b. Ontogeny of worker body size distribution in bumble bee (*Bombus impatiens*) colonies. Ecol. Entomol. 35: 424–435.

Daly, H. V., K. Hoelmer, and P. Gambino. 1991. Clinal geographic variation in feral honey bees in California, USA. Apidologie 22: 591–609.

Danecek, P., A. Auton, G. Abecasis, C. A. Albers, E. Banks, M. A. DePristo, R. E. Handsaker, G. Lunter, G. T. Marth, S. T. Sherry, et al. 2011. The variant call format and VCFtools. Bioinformatics 27: 2156–2158.

Dillon, M. E., and R. Dudley. 2004. Allometry of maximum vertical force production during hovering flight of neotropical orchid bees (Apidae: Euglossini). J. Exp. Biol. 207: 417–425.

Dillon, M. E., and R. Dudley. 2014. Surpassing Mt. Everest: extreme flight performance of alpine bumble-bees. Biol. Lett. 10: 20130922–20130922.

Dillon, M. E., and M. R. Frazier. 2006. *Drosophila melanogaster* locomotion in cold thin air. J. Exp. Biol. 209: 364–371.

Dillon, M. E., M. R. Frazier, and R. Dudley. 2006. Into thin air: physiology and evolution of alpine insects. Integr. Comp. Biol. 46: 49–61.

Dudley, R. 2000. The biomechanics of insect flight: form, function, evolution. Princeton University Press, Princeton, NJ.

Dudley, R., and C. Ellington. 1990. Mechanics of forward flight in bumblebees: I. Kinematics and morphology. J. Exp. Biol. 148: 19–52.

Duennes, M. A., J. D. Lozier, H. M. Hines, and S. A. Cameron. 2012. Geographical patterns of genetic divergence in the widespread Mesoamerican bumble bee *Bombus ephippiatus* (Hymenoptera: Apidae). Mol. Phylogenet. Evol. 64: 219–231.

Foster, D. J., and R. V. Cartar. 2011. What causes wing wear in foraging bumble bees? J. Exp. Biol. 214: 1896–1901.

Frazier, M. R., H. A. Woods, and J. F. Harrison. 2001. Interactive effects of rearing temperature and oxygen on the development of *Drosophila melanogaster*. Physiol. Biochem. Zool. 74: 641–650.

Frazier, M. R., J. F. Harrison, S. D. Kirkton, and S. P. Roberts. 2008. Cold rearing improves cold-flight performance in *Drosophila* via changes in wing morphology. J. Exp. Biol. 211: 2116–2122.

Gérard, M., M. Vanderplanck, M. Franzen, M. Kuhlmann, S. G. Potts, P. Rasmont, O. Schweiger, and D. Michez. 2018. Patterns of size variation in bees at a continental scale: does Bergmann's rule apply? Oikos 127: 1095–1103.

Ghisbain, G., J. D. Lozier, S. R. Rahman, B. D. Ezray, L. Tian, J. M. Ulmer, S. D. Heraghty, J. P. Strange, P. Rasmont, and H. M. Hines. 2020. Substantial genetic divergence and lack of recent gene flow support cryptic speciation in a colour polymorphic bumble bee (*Bombus bifarius*) species complex. Syst. Entomol. 45: 635–652.

Gilchrist, G. W., and R. B. Huey. 2004. Plastic and genetic variation in wing loading as a function of temperature within and among parallel clines in *Drosophila subobscura*. Integr. Comp. Biol. 44: 461–70.

Goslee, S. C., and D. L. Urban. 2007. The ecodist package for dissimilarity-based analysis of ecological data. J. Stat. Softw. 22: 1–19.

Goudet, J., and T. Jombart. 2018. hierfstat: estimation and tests of hierarchical F-statistics. R package version 0.04-30.

Goulson, D. 2010. Bumblebees: behaviour, ecology, and conservation. Oxford University Press, New York.

Greenleaf, S. S., N. M. Williams, R. Winfree, and C. Kremen. 2007. Bee foraging ranges and their relationship to body size. Oecologia 153: 589–96.

Hagen, M., and Y. L. Dupont. 2013. Inter-tegular span and head width as estimators of fresh and dry body mass in bumblebees (*Bombus* spp.). Insectes Soc. 60: 251–257.

Harrison, J. F., A. Kaiser, and J. M. VandenBrooks. 2010. Atmospheric oxygen level and the evolution of insect body size. Proc. R. Soc. B Biol. Sci. 277: 1937–1946.

Harrison, X. A., L. Donaldson, M. E. Correa-Cano, J. Evans, D. N. Fisher, C. E. D. Goodwin, B. S. Robinson, D. J. Hodgson, and R. Inger. 2018a. A brief introduction to mixed effects modelling and multi-model inference in ecology. PeerJ 2018: 1–32.

Harrison, J. F., K. J. Greenlee, and W. C. E. P. Verberk. 2018b. Functional hypoxia in insects: definition, assessment, and consequences for physiology, ecology, and evolution. Annu. Rev. Entomol. 63: 303–325.

Heinrich, B. 1975. Thermoregulation in bumblebees. J. Comp. Physiol. B Biochem. Syst. Environ. Physiol. 96: 155–166.

Heinrich, B. 1976. Heat exchange in relation to blood flow between thorax and abdomen in bumblebees. J. Exp. Biol. 64: 561–85.

Heinrich, B. 1977. The physiology of exercise in the bumblebee. Am. Sci. 65: 455–465.

Heinrich, B. 2004. Bumblebee economics. Harvard University Press, Cambridge, MA.

Heinrich, B., and A. E. Kammer. 1973. Activation of the fibrillar muscles in the bumblebee during warm-up, stabilization of thoracic temperature and flight. J. Exp. Biol. 58: 677–688.

Hepburn, H. R., C. Youthed, P. Illgner, S. E. Radloff, and R. E. Brown. 1998. Production of aerodynamic power in mountain honeybees (*Apis mellifera*). Naturwissenschaften 85: 389–390.

Heraghty, S. D., J. M. Sutton, M. L. Pimsler, J. L. Fierst, J. P. Strange, and J. D. Lozier. 2020. De novo genome assemblies for three North American bumble bee species: *Bombus bifarius*, *Bombus vancouverensis*, and *Bombus vosnesenskii*. G3. 10: 2585–2592.

Hijmans, R. J. 2019. geosphere: spherical trigonometry. R package version 1.5-10.

Hijmans, R. J. 2020. raster: geographic data analysis and modeling. R package version 3.0-12.

Hijmans, R. J., S. E. Cameron, J. L. Parra, P. G. Jones, and A. Jarvis. 2005. Very high resolution interpolated climate surfaces for global land areas. Int. J. Climatol. 25: 1965–1978.

Hines, H. M., and P. H. Williams. 2012. Mimetic colour pattern evolution in the highly polymorphic *Bombus trifasciatus* (Hymenoptera: Apidae) species complex and its comimics. Zool. J. Linn. Soc. 166: 805–826.

Hodkinson, I. D. 2005. Terrestrial insects along elevation gradients: species and community responses to altitude. Biol. Rev. 80: 489.

Horne, C. R., A. G. Hirst, and D. Atkinson. 2018. Insect temperature–body size trends common to laboratory, latitudinal and seasonal gradients are not found across altitudes. Funct. Ecol. 32: 948–957.

Hunt, G. J., E. Guzmán-Novoa, M. K. Fondrk, and R. E. Page. 1998. Quantitative trait loci for honey bee stinging behavior and body size. Genetics 148: 1203–13.

Jackson, J. M., M. L. Pimsler, K. J. Oyen, J. B. Koch-Uhuad, J. D. Herndon, J. P. Strange, M. E. Dillon, and J. D. Lozier. 2018. Distance, elevation and environment as drivers of diversity and divergence in bumble bees across latitude and altitude. Mol. Ecol. 27: 2926–2942.

Jackson, J. M., M. L. Pimsler, K. J. Oyen, J. P. Strange, M. E. Dillon, and J. D. Lozier. 2020. Local adaptation across a complex bioclimatic landscape in two montane bumble bee species. Mol. Ecol. 29: 920–939.

James, F. C. 1970. Geographic size variation in birds and its relationship to climate. Ecology 51: 365–390.

Kawecki, T. J., and D. Ebert. 2004. Conceptual issues in local adaptation. Ecol. Lett. 7: 1225–1241.

Kelemen, E. P., G. Davidowitz, and A. Dornhaus. 2020. Size variation does not act as insurance in bumble bees; instead, workers add weight in an unpredictable environment. Anim. Behav. 170: 99–109.

Keller, I., J. M. Alexander, R. Holderegger, and P. J. Edwards. 2013. Widespread phenotypic and genetic divergence along altitudinal gradients in animals. J. Evol. Biol. 26: 2527–2543.

Kendall, L. K., R. Rader, V. Gagic, D. P. Cariveau, M. Albrecht, K. C. R. Baldock, B. M. Freitas, M. Hall, A. Holzschuh, F. P. Molina, et al. 2019. Pollinator size and its consequences: robust estimates of body size in pollinating insects. Ecol. Evol. 9: 1702–1714.

Kerr, J. T., A. Pindar, P. Galpern, L. Packer, S. G. Potts, S. M. Roberts, P. Rasmont, O. Schweiger, S. R. Colla, L. L. Richardson, et al. 2015. Climate change impacts on bumblebees converge across continents. Science 349: 177–180.

Klepsatel, P., M. Gáliková, C. D. Huber, and T. Flatt. 2014. Similarities and differences in altitudinal versus latitudinal variation for morphological traits in *Drosophila melanogaster*. Evolution 68: 1385–1398.

Kuznetsova, A., P. B. Brockhoff, and R. H. B. Christensen. 2017. lmerTest package: tests in linear mixed effects models. J. Stat. Softw. 82: 1–26.

Legendre, P., F.-J. Lapointe, and P. Casgrain. 1994. Modeling brain evolution from behavior: a permutational regression approach. Evolution 48: 1487.

López-Uribe, M. M., S. Jha, and A. Soro. 2019. A trait-based approach to predict population genetic structure in bees. Mol. Ecol. 28: 1919–1929.

Lozier, J. D., J. P. Strange, I. J. Stewart, and S. A. Cameron. 2011. Patterns of range-wide genetic variation in six North American bumble bee (Apidae: *Bombus*) species. Mol. Ecol. 20: 4870–4888.

Lozier, J. D., J. M. Jackson, M. E. Dillon, and J. P. Strange. 2016. Population genomics of divergence among extreme and intermediate color forms in a polymorphic insect. Ecol. Evol. 6: 1075–1091.

Lüdecke, D. 2020. sjPlot: data visualization for statistics in social science. R package version 2.9.2.

Mayr, E. 1956. Geographical character gradients and climatic adaptation. Evolution 10: 105–108.

McCulloch, G. A., and J. M. Waters. 2018. Does wing reduction influence the relationship between altitude and insect body size? A case study using New Zealand's diverse stonefly fauna. Ecol. Evol. 8: 953–960.

Mola, J. M., M. R. Miller, S. M. O'Rourke, and N. M. Williams. 2020. Forests do not limit bumble bee foraging movements in a montane meadow complex. Ecol. Entomol. 45: 955–965.

Mountcastle, A. M., T. M. Alexander, C. M. Switzer, and S. A. Combes. 2016. Wing wear reduces bumblebee flight performance in a dynamic obstacle course. Biol. Lett. 12: 1–4.

Nijhout, H. F., and V. Callier. 2015. Developmental mechanisms of body size and wing-body scaling in insects. Annu. Rev. Entomol. 60: 141–156.

Norry, F. M., O. A. Bubliy, and V. Loeschcke. 2001. Developmental time, body size and wing loading in *Drosophila buzzatii* from lowland and highland populations in Argentina. Hereditas 135: 35–40.

Oyen, K. J., S. Giri, and M. E. Dillon. 2016. Altitudinal variation in bumble bee (*Bombus*) critical thermal limits. J. Therm. Biol. 59: 52–57.

Peat, J., B. Darvill, J. Ellis, and D. Goulson. 2005. Effects of climate on intra- and interspecific size variation in bumble-bees. Funct. Ecol. 19: 145–151.

Pesevski, M., and I. Dworkin. 2020. Genetic and environmental canalization are not associated among altitudinally varying populations of *Drosophila melanogaster*. Evolution 74: 1755–1771.

Peterman, W. E. 2018. ResistanceGA: an R package for the optimization of resistance surfaces using genetic algorithms. Methods Ecol. Evol. 9: 1638–1647.

Peterman, W. E., G. M. Connette, R. D. Semlitsch, and L. S. Eggert. 2014. Ecological resistance surfaces predict fine-scale genetic differentiation in a terrestrial woodland salamander. Mol. Ecol. 23: 2402–2413.

Pimsler, M. L., K. J. Oyen, J. D. Herndon, J. M. Jackson, J. P. Strange, M. E. Dillon, and J. D. Lozier. 2020. Biogeographic parallels in thermal tolerance and gene expression variation under temperature stress in a widespread bumble bee. Sci. Rep. 10: 17063.

Pitchers, W., J. E. Pool, and I. Dworkin. 2013. Altitudinal clinal variation in wing size and shape in African *Drosophila melanogaster*: one cline or many? Evolution 67: 438–52.

R Core Team. 2019. R: a language and environment for statistical computing.

Ramírez-Delgado, V. H., S. Sanabria-Urbán, M. A. Serrano-Meneses, and R. Cueva del Castillo. 2016. The converse to Bergmann's rule in bumblebees, a phylogenetic approach. Ecol. Evol. 6: 6160–6169.

Revelle, W. 2019. psych: procedures for psychological, psychometric, and personality research. R package version 1.9.12.31.

Rousset, F., and J.-B. Ferdy. 2014. Testing environmental and genetic effects in the presence of spatial autocorrelation. Ecography 37: 781–790.

Schneider, C. A., W. S. Rasband, and K. W. Eliceiri. 2012. NIH image to ImageJ: 25 years of image analysis. Nat. Methods 9: 671–675.

Scriven, J. J., P. R. Whitehorn, D. Goulson, and M. C. Tinsley. 2016. Bergmann's body size rule operates in facultatively endothermic insects: evidence from a complex of cryptic bumblebee species. PLoS ONE 11: 1–11.

Shah, A. A., M. E. Dillon, S. Hotaling, and H. A. Woods. 2020. High elevation insect communities face shifting ecological and evolutionary landscapes. Curr. Opin. Insect Sci. 41: 1–6.

Shelomi, M. 2012. Where are we now? Bergmann's rule sensu lato in insects. Am. Nat. 180: 511–519.

Sirois-Delisle, C., and J. T. Kerr. 2018. Climate change-driven range losses among bumblebee species are poised to accelerate. Sci. Rep. 8: 14464.

Slatyer, R. A., S. D. Schoville, C. R. Nufio, and L. B. Buckley. 2019. Do different rates of gene flow underlie variation in phenotypic and phenological clines in a montane grasshopper community? Ecol. Evol. 10: 1–18.

Vogt, J. R., and M. E. Dillon. 2013. Allometric scaling of tracheal morphology among bumblebee sisters (Apidae: *Bombus*): compensation for oxygen limitation at large body sizes? Physiol. Biochem. Zool. 86: 576–587.

Whitlock, M. C., and F. Guillaume. 2009. Testing for spatially divergent selection: comparing QST to FST. Genetics 183: 1055–63.

Wickham, H. 2016. ggplot2: elegant graphics for data analysis. Springer-Verlag, New York.

Williams, P. H., J. M. Lobo, and A. S. Meseguer. 2018. Bumblebees take the high road: climatically integrative biogeography shows that escape from Tibet, not Tibetan uplift, is associated with divergences of present-day *Mendacibombus*. Ecography 41: 461–477.

Woods, H. A. 2004. Temperature-dependent oxygen limitation in insect eggs. J. Exp. Biol. 207: 2267–2276.